

## *Vacuum Ultraviolet Absorption Spectra of Saturated Organic Compounds with Non-bonding Electrons*

By Hiroshi TSUBOMURA,\* Katsumi KIMURA,\* Koji KAYA,  
Jiro TANAKA and Saburo NAGAKURA

(Received November 7, 1963)

The electronic spectra of aliphatic compounds have received relatively little attention from organic chemists because they lie mostly in the vacuum ultraviolet region. Saturated compounds containing non-bonding electron pairs like alcohols, ethers, amines, and halides show characteristic absorption bands in the region between 1600 and 2000 Å, the investigation of which seems to be important for a theoretical understanding of the electronic structures of these compounds. These bands may be important also for the chemical analysis of these compounds.

Most of the spectral measurements in the vacuum ultraviolet region have been made with the photographic method. About ten years ago, Kleven and Platt<sup>1)</sup> measured the spectra of various aliphatic and aromatic compounds in the vacuum ultraviolet region up to 1750 Å. A group at Mount Holyoke College has also measured the vacuum ultraviolet

absorption spectra of many aliphatic compounds, including olefins, aliphatic amines and alcohols.<sup>2,3)</sup>

Photoelectric measurements of the vacuum ultraviolet spectra have been carried out by Watanabe and others.<sup>4)</sup> Most of their work, however, has been on very simple molecules. Recently, some automatic recording spectrophotometers have become commercially available with which the measurements can be extended down to 1850 or even 1750 Å. Kaye<sup>5)</sup> has done work by a commercially-available instrument on some alcohols and has found that their spectra shift to the blue as a result of the hydrogen bonding. Under these circumstances, the present authors undertook to construct a recording spectrophotometer suitable

\* Present address: Department of Chemistry, Faculty of Engineering Science, Osaka University, Toyonaka, Osaka.

1) H. B. Kleven and J. R. Platt, "Technical Report of Laboratory of Molecular Structure and Spectra, Dept. Phys., University of Chicago," (1953-1954).

2) J. T. Gary and L. W. Pickett, *J. Chem. Phys.*, **22**, 599, 1226 (1954).

3) E. Tannenbaum, E. M. Coffin and A. J. Harrison, *J. Chem. Phys.*, **21**, 311 (1953).

4) K. Watanabe, M. Zelickoff and E. C. Y. Inn, Geophysics Research Papers 21. AFCRC Technical Report No. 53-23, Geophysics Research Directorate, Air Force Cambridge Research Center, 1953.

5) W. B. Kaye and R. E. Poulson, *Nature*, **193**, 675 (1962); also 13th Pittsburgh Conference on Anal. Chem. and Applied Spectroscopy., 1962.

for the accurate measurement of absorption intensity in the vacuum ultraviolet region from 1450 to 2200 Å, and to measure the vacuum ultraviolet absorption spectra of some saturated organic compounds with non-bonding electrons, such as alcohols, ether, amines and chlorides.

Mulliken was the first to give a theoretical explanation of the spectra of aliphatic alcohols, amines and halides. In his early-published paper,<sup>6a)</sup> he explained that the near vacuum ultraviolet absorption bands of these compounds may be attributed to the Rydberg-type transition from the lone pair  $np$  atomic orbital to the vacant  $(n+1)s$  atomic orbital. Later, he pointed out that these bands are more likely to be of the  $n \rightarrow \sigma^*$  type, because of the transition from the non-bonding atomic orbital (abbreviated hereafter to AO) to the vacant  $\sigma$ -antibonding molecular orbital (abbreviated hereafter to MO), although the possibility of the Rydberg nature of these bands can not be entirely excluded.<sup>6b)</sup> The present authors intend to give a more detailed theoretical interpretation of the nature of these bands.

### Experimental

The near ultraviolet absorption spectra ( $\lambda > 1900$  Å) were measured with a Cary model 14M spectrophotometer, while the spectra in the region of wavelengths shorter than 2200 Å were measured by a vacuum ultraviolet spectrophotometer constructed in our laboratory. The instrument, shown diagrammatically in Fig. 1, is more or less similar to the one constructed by Watanabe and Inn.<sup>7)</sup>

The spectrophotometer uses a Bausch & Lomb concave grating (catalog No. 33-52-25-41; concave radius 995.4 mm., ruled area 56 mm.  $\times$  96 mm., 600 grooves/mm., blazed at 1500 Å, blaze angle  $2^\circ 35'$ ). The center of the grating and the two slits  $S_1$  and  $S_2$  are on the Rowland circle (with the diameter equal to the concave radius), so the light from the entrance slit,  $S_1$ , is always focused at the exit slit,  $S_2$ . The grating holder is fixed on a steel ball at the center of the circle and has two small rollers under the grating. It also has a vertical lever which is pushed by a micrometer head for scanning. The micrometer has a pitch of 0.5 mm. and is rotated by a synchronous motor through a gear set at speeds of 2, 4 and 8 rotations per minutes. The wavelength changes by about 45 Å per each rotation.

Hydrogen-discharge lamps from Hitachi, Ltd. and the Asahidenko Co. were used as light sources. They are hot-cathode type lamps with working voltages of 60 to 100 V. and a current of about 1 amp. Each of these lamps has a specially-designed power supply; further, a voltage stabilizer was used. The lamp has an optically-flat fused silica

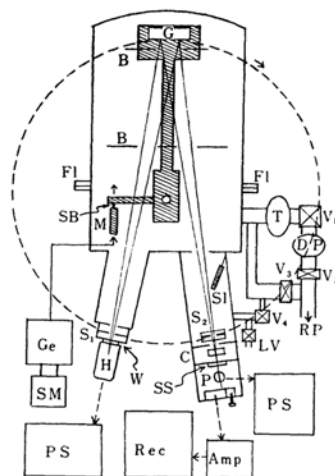


Fig. 1. Block diagram of the vacuum ultraviolet spectrophotometer. G, Grating; B, Baffle; Fl, Flange; SB, Steel ball; M, Micrometer; Sl, Shutter;  $S_1$ ,  $S_2$ , Slits; H, Hydrogen discharge lamp; W, Lithium fluoride window; C, Cell; SS, A glass plate coated with sodium salicylate; P, Photomultiplier; Z, Zero adjuster; PS, Power supply; Amp, Amplifier; Rec, Recorder; SM, Synchronous motor; Ge, Gear set; LV, Leak valve;  $V_1$ ,  $\sim V_6$ , Valves; T, Cold trap; Dp, Diffusion pump; RP, Rotary pump

window which is pushed against the lithium fluoride window (also optically-flat) in front of the entrance slit of the monochromator so as to minimize the air gap between them.

The shutter designated by Sl in Fig. 1 can be operated from outside and serves both as a light shutter and a vacuum valve to insulate the cell compartment from the main body of the monochromator. Each of the cells is cemented with Araldite to the cover plate, which is fixed in position at the flange of the cell compartment when it is in use (see Fig. 2). Such cell assemblies can be exchanged for various purposes after filling the cell compartment with air by operating the shutter, Sl, the valves LV, and other parts.

The light passing through the cell finally hits a glass window cemented on the outer surface of the cell compartment. The inner surface of the glass is covered with a thin layer of sodium salicylate, and the fluorescence caused by the vacuum ultraviolet light is received by a RCA 1P28 photomultiplier tube. The output is amplified by a DC microammeter of the Ohkura Electric Co. and recorded by a Brown recorder. A zero adjuster consisting of a battery and a variable resistance is also connected.

The monochromator tank consists of two parts, which are joined together with bolts and nuts at the flanges. The rear part of the tank has rollers under it and can be moved along the rail when service is needed for the inside of the monochromator.

6) a) R. S. Mulliken, *Phys. Rev.*, **47**, 413 (1935); b) R. S. Mulliken, *J. Chem. Phys.*, **8**, 382 (1940); *Phys. Rev.*, **61**, 277 (1942).

7) K. Watanabe and E. C. Y. Inn, *J. Opt. Soc. Am.*, **43**, 32 (1953).

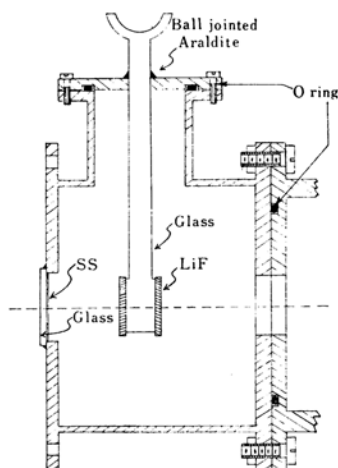


Fig. 2. The cell compartment and the vapor cell.

Figure 2 shows one of the cells for vapor measurement; they are made of glass and have two lithium fluoride windows cemented with Araldite. The inner thickness of the cell ranges from 7 to 30 mm. Each of the cells is connected with a vacuum line with a ball joint and is evacuated. The hydrogen lamp emission intensity is recorded under these conditions for use as reference. The sample vapor is then introduced, and the pressure is measured with a mercury manometer with an inner diameter of 20 mm. The mercury level is read with a measuring microscope. The sensitivity of the pressure reading is about 0.01 mm. The emission intensity is recorded for the sample. In Fig. 3, the measured curve for ethanol is given as a typical example of vapor measurements. Curve A is for the reference, curve B for the sample, and curve C for the molar extinction calculated from the two former curves. The short vertical lines on curves A and B are wavelength markers, given by the short-circuiting of the recorder input voltage at each rotation of the wavelength-drive micrometer. This is actually done by a microswitch in contact with the micrometer drum, which has a small cut at the periphery. The calibration of the wavelength has been done by comparing the marker readings recorded on the chart and the peak wavelengths of the absorption spectra of a certain number of compounds, for instance, acetone, whose peak wavelengths have been given in an earlier work.

As shown in the figure, the intensity of the emission of the hydrogen lamp decreases gradually in the vacuum ultraviolet region, reaching a minimum at about 1700 Å. Then it rises because of the atomic emission, falls very steeply because of the absorption of fused silica, and becomes almost flat below 1500 Å. In the flat region the intensity of the monochromatized light must be zero; hence, it gives the intensity of the stray light. We therefore call it the stray level. The final falling of the curve corresponds to the shutting off of the shutter, Sl. From the flatness of the stray level below 1500 Å, one may assume that the intensity of the

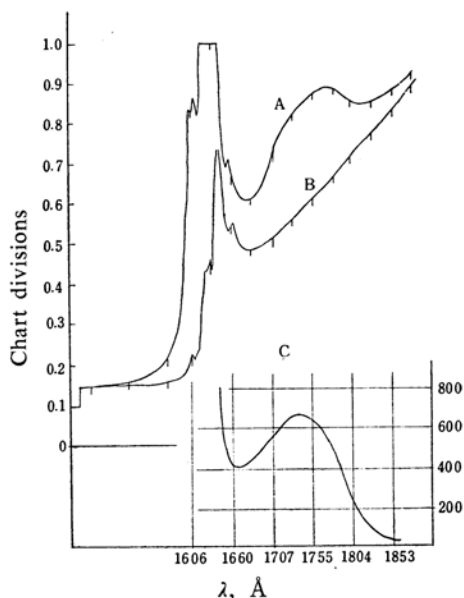


Fig. 3. Recorded curves for ethanol. A, Reference recording; B, Sample recording; C, The curve calculated from A and B (See text).

stray light is nearly constant in the wavelength range we are interested in. Therefore, by taking the "stray level" appearing in the curve to be the zero line, we can calculate the absorbance,  $\log_{10}(I_0/I)$ , from the curves for the reference and the sample. The effect of stray light can thus be reduced to less than a few percent. The extinction coefficients at about 2000 Å measured with this instrument agree well with those measured with the Cary 14 M spectrophotometer, the differences being in most cases less than 10%.

For solution measurements, fused silica cells, an example of which is depicted in Fig. 4, (made by the Nihon Sekiei Co.) were used. The inner thickness is about 0.1 mm. This seems to be the technically available lower limit for the precise

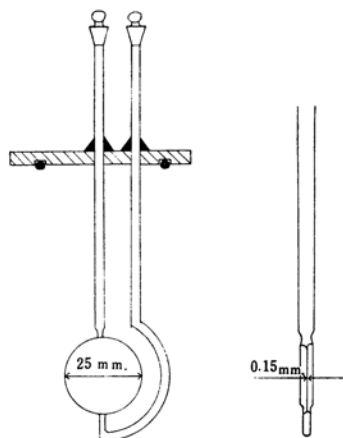


Fig. 4. The solution cell.

TABLE I. THE OBSERVED CHARACTERISTICS OF THE ULTRAVIOLET BANDS

| Compound             | $\lambda_{\max}$ , Å | $\epsilon_{\max}$ , l./mol. cm. | $\Delta\nu_{1/2}$ , $\text{cm}^{-1}$ | $f$    |
|----------------------|----------------------|---------------------------------|--------------------------------------|--------|
| a) Oxygen compound   |                      |                                 |                                      |        |
| Water                | 1670                 | 2120                            | 9100                                 | 0.084  |
| Methanol             | 1742                 | 356                             | 3400                                 | 0.0052 |
| Ethanol              | 1740                 | 670                             | 4400                                 | 0.013  |
| Ethyl ether          | 1885                 | 2820                            | 3400                                 | 0.041  |
| b) Amine             |                      |                                 |                                      |        |
| Triethylamine        | 2120                 | 6100                            | 8400                                 | 0.22   |
| c) Chloride          |                      |                                 |                                      |        |
| Methyl chloride      | 1690                 | 370                             | 6500                                 | 0.010  |
| Dichloromethane      | 1790                 | 510                             | —                                    | —      |
| Chloroform           | 1755                 | 950                             | 6400                                 | 0.026  |
| Carbon tetrachloride | 1740                 | 2370                            | 6200                                 | 0.063  |

construction of such cells. The thickness was calibrated by measurements of the absorption spectrum of a *n*-heptane solution of chlorobenzene with the Cary spectrophotometer. Even with such thin cells, the absorption by the solvents is enormous, and purified *n*-heptane has turned out to be the only solvent which can be used in this range, though some other homologues can probably be so used also.

### Results and Discussion

**Water, Alcohol and Ether.**—Figures 5 and 6 and Table Ia give the results for the spectra of water, alcohols and ether. The spectral shapes obtained are in good agreement with those of Harrison et al.<sup>8,9)</sup> and with those of Watanabe and Zelikoff,<sup>10)</sup> although our molar

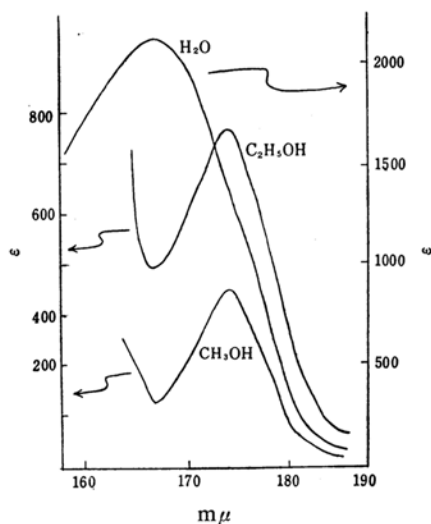


Fig. 5. The absorption spectra for water, methanol and ethanol.

extinction values are 1.5 times to twice as large as theirs. The reason for this discrepancy is not clear.

The experimental results seem to be explained reasonably by the following assumption (see Fig. 7): 1) These bands are essentially of the  $n \rightarrow \sigma^*$  type, where  $n$  means the 2p AO of the oxygen atom directed along the line perpendicular to the molecular plane; 2) the  $\sigma^*$

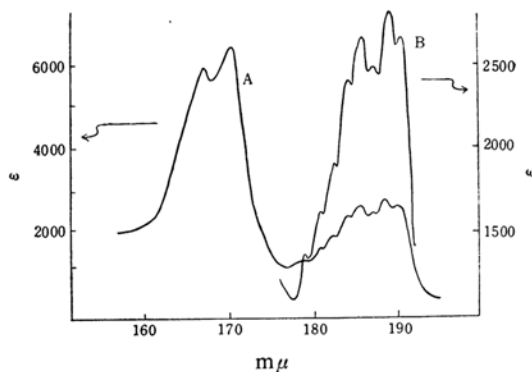


Fig. 6. The spectrum for ether. Curve B is for an expanded scale.

orbital for the C-O bond,  $\sigma^*(\text{CO})$ , has an orbital energy appreciably lower than that for the  $\sigma^*(\text{OH})$  orbital (the reason for this will be given later), and 3) the matrix elements of the Hamiltonian between two  $\sigma^*$  orbitals in a molecule are small (see the Appendix). Therefore, the two upper configurations,  $n \rightarrow \sigma^*(\text{OH})$  and  $n \rightarrow \sigma^*(\text{CO})$ , in alcohols interact slightly, while the two  $n \rightarrow \sigma^*$  configurations of water and ether interact strongly with each other, because they are degenerate. If the

8) A. J. Harrison, B. J. Cederholm and M. A. Terwillinger, *J. Chem. Phys.*, **30**, 355 (1959).

9) A. J. Harrison and D. R. W. Price, *ibid.*, **30**, 357 (1959).

10) K. Watanabe and M. Zelikoff, *J. Opt. Soc. Am.*, **43**, 753 (1953).

\* It may be expected that the electron affinity of a molecule generally gets larger as the molecule becomes larger, because the extra charge is more or less stabilized by the polarization of other electrons in the molecules. Therefore, the transition energy may conceivably be affected by the electron affinity, too, but its effect may be smaller than the effect of the ionization potential.

energy levels of the molecular states are approximated by the relevant orbital energies, the lower levels shown in Fig. 7 correspond to the orbital energies of the oxygen non-bonding orbitals, which are taken to be equal to the ionization potentials for these molecules (with the sign reversed). The upper levels correspond to the orbital energies of the  $\sigma^*$  (antibonding) molecular orbitals. The differences in energies between the two levels are taken to be equal to the observed transition energies.

From Fig. 7 it may be seen that the transition energy increases in the order of  $(\text{C}_2\text{H}_5)_2\text{O} < \text{C}_2\text{H}_5\text{OH} < \text{H}_2\text{O}$ . The transition energy corresponds roughly to  $(I - A - Q)$ , where  $I$  is the ionization potential of the molecule,  $A$  is the electron affinity associated with the  $\sigma^*$  orbital, and  $Q$  is the electrostatic energy due to the charge unbalance in the upper state. Moreover, the ionization potential value undoubtedly increases in the following order;  $(\text{C}_2\text{H}_5)_2\text{O} < \text{C}_2\text{H}_5\text{OH} < \text{H}_2\text{O}$ . Thus, we can explain the fact the  $n \rightarrow \sigma^*$  band shifts toward shorter wavelengths in the order of ether, alcohol and water.\* The reason why ether absorbs at longer wavelengths than alcohol may be partly attributed to the splitting of the antibonding  $\sigma^*$  orbital in the former.

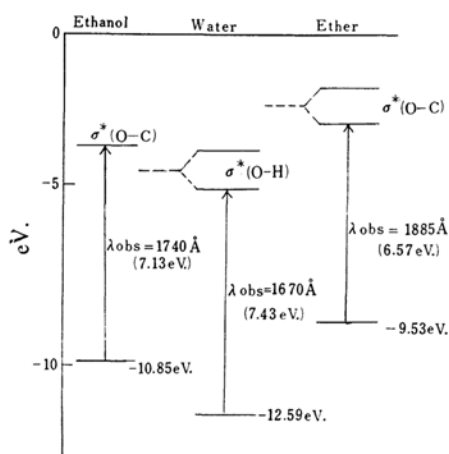


Fig. 7. The energy levels of ethanol, water and ether.

The oscillator strength of a transition,  $f$ , is related to the transition moment,  $\mu$  (in Debye units), by the following equation;

$$f = 8\pi^2 \nu_{\max} m \mu^2 / 3h^2 e^2 = 4.704 \times 10^{-7} \nu_{\max} \mu^2 \quad (1)$$

where  $\nu_{\max}$  (in  $\text{cm}^{-1}$ ) is the wave number at the maximum,  $m$  and  $e$  are the mass and the charge of an electron, and  $h$  is Planck's constant. The transition moment for the  $n \rightarrow \sigma^*$  (CO) transition can be expressed by the present scheme as follows:

$$\mu = \int \psi(n)(ex)\psi^*(\sigma)dv = \int \psi_{2px_0} \times (ex)(a\psi_{2pz_0} - b\psi_c)dv = b \int \psi_{2px_0}(ex)\psi_c dv \quad (2)$$

where  $a$  and  $b$  are normalized coefficients for the  $\sigma^*$  MO,  $z$  is directed along the bond, and  $x$  is vertical to the molecular plane.  $\psi_c$  is an  $\text{sp}^3$ -hybridized AO directing the bond. Calculation by the use of the Slater AO's leads to  $\mu = 0.74b$  in Debye units. If one assumes that  $a = b$ ,  $f$  is calculated to be of the order of 0.011, a value which is in good agreement with the experimental value for alcohols. On the other hand, if the upper MO is assumed to be  $\sigma^*(\text{OH}) = a'\psi_{2pz_0} - b'\psi_{1sH}$ , the transition moment is given by  $\mu' = b' \int \psi_{2px_0}$

$(ex)\psi_{1sH}dv$ . The result is  $\mu = 3.0$  D and  $f = 0.24$ . The  $f$  value obtained is 20 times larger than the observed  $f$  values for alcohols. Therefore, it can be concluded that the upper MO for the case of alcohols is more likely to be  $\sigma^*(\text{CO})$ .

In the water and ether molecules, the two  $\sigma^*$  orbitals interact with each other, resulting in two MO's;

$$\begin{aligned} \phi_1 &= 2^{-1/2} \{ \sigma^*(\text{OX}_1) + \sigma^*(\text{OX}_2) \} \\ \phi_2 &= 2^{-1/2} \{ \sigma^*(\text{OX}_1) - \sigma^*(\text{OX}_2) \} \end{aligned} \quad (3)$$

The symmetric combination  $\phi_1$  will have the lower energy. By inspection one can easily see that  $\phi_1$  is equivalent to the first vacant SCF MO of water as calculated by Ellison Shull.<sup>11)</sup> The transition moment in this case is then given by

$$\begin{aligned} \mu_{n\phi_1} &= 2^{-1/2} \left\{ \int \psi(n)(ex)\sigma^*(\text{OX}_1)dv \right. \\ &\quad \left. + \int \psi(n)(ex)\sigma^*(\text{OX}_2)dv \right\} \end{aligned} \quad (4)$$

The two terms in the brackets have directions parallel to each other, and their magnitudes are same. Hence,

$$\mu_{n\phi_1} = 2^{1/2} \int \psi(n)(ex)\sigma^*(\text{OX}_1)dv \quad (5)$$

Therefore, the  $n \rightarrow \phi_1$  transition has a probability twice as large as that of the  $n \rightarrow \sigma^*$  transition in alcohols, and that of  $n \rightarrow \phi_2$  is impossible.

In this way we can explain the experimental result that the symmetric molecule (ether) has stronger absorption bands than asymmetric molecules (alcohols). Also, the larger calculated  $f$  value for the  $n \rightarrow \sigma^*(\text{OH})$  transition may explain the experimental  $f$  value for water larger than that for ether. Thus, it can be seen that the transition scheme proposed above explains the qualitative characteristics of observed bands, although a more quantitative agreement between theory and observed

results can not be expected from such a simple treatment.

According to the above treatment,  $\mu_{n\psi_2}$  becomes zero. The second absorption band of ether observed by us and also by Harrison and Price at about  $1700\text{\AA}$  has an intensity larger than that of the first band. It is, therefore, concluded to be due to another transition, and the  $n \rightarrow \psi_2$  band may be hidden in it.

**Amine.**—The lone pair AO of the nitrogen atom in alkyl amines and ammonia is thought

to be the (s, p)-hybridized AO, directed along the symmetry axis or pseudo-symmetry axis of the pyramidal molecules. Therefore, it can easily be seen that the  $n \rightarrow \sigma^*$  transition has a fairly strong intensity, since the transition moment integral contains not only the two center terms, such as appear in Eq. 2, but also the one center terms, like

$$\int \psi_{2pxN}(ex)\psi_{2sNd}v, \text{ which is quite large.}$$

Our experimental result on the vapor spectrum of triethylamine has shown that its  $f$  value is indeed of an order of magnitude higher than that for alcohols (see Table I).

**Chlorides.**—Figure 8 and Table Ic show the experimental results obtained for the four chlorides of methane. The  $\epsilon$  and  $f$  values for methyl chloride are of an order of magnitude equal to those for alcohols, and to those for bromides and iodides measured by Kimura and Nagakura.<sup>12)</sup> Hence, it seems reasonable to assume that the transition is  $n \rightarrow \sigma^*$ , where  $n$  is the  $3px$  AO of chlorine and  $\sigma^*$  is the antibonding MO for the C-Cl bond.

In polychlorides, there are a number of  $n$  and  $\sigma^*$  orbitals. Theoretically, these orbitals should not interact strongly with each other. Hence, the absorption intensities, or  $f$  values, for polychlorides must be approximately proportional to the number of chlorine atoms when the axes of the  $n$  AO's of the Cl atoms are assumed to be all parallel. The experimental results show that the  $f$  values increase approximately at the predicted rate.

The observed spectra of polychlorides show rather complicated features, suggesting that these spectra consist of a certain number of divided bands, as was observed in the case of bromides and iodides.<sup>12)</sup> However, the splitting in the present case appears to be much smaller, indicating that the interactions between orbitals belonging to different C-X bonds are smaller in this case.

**Comment on the Rydberg Nature of the Transitions.**—It is clear that the vacuum ultraviolet bands discussed above are more or less of a *molecular* nature, because they are rather sensitive to the atoms or groups of atoms to which the central atom is bonded. In this sense, it is definitely erroneous to conclude simply that these bands are due to transitions from AO's  $np$  to  $(n+1)s$ , with the energies of these AO's independent of the other components of the molecules.

Kimura and Nagakura<sup>12)</sup> calculated the

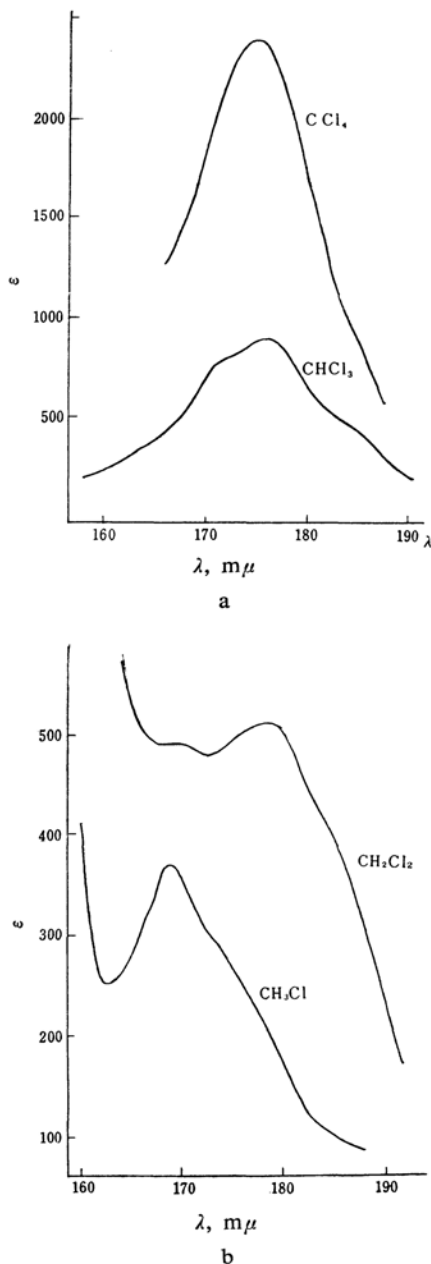


Fig. 8. Spectra for the chlorides of methane.

11) F. O. Ellison and H. Shull, *J. Chem. Phys.*, **23**, 2348 (1955).

12) K. Kimura and S. Nagakura, *Spectrochim. Acta*, **17**, 166 (1961).

oscillator strengths of the  $np \rightarrow (n+1)s$  transitions for bromides and iodides and showed that the calculated values were much higher than the observed values. For this reason the bands were concluded to be of the  $n \rightarrow \sigma^*$  nature.

The calculated oscillator strength for the  $np \rightarrow (n+1)s$  transition generally gets smaller as  $n$  becomes smaller. For the  $2p \rightarrow 3s$  transition of the oxygen atom, the calculation leads to  $f=0.01$ , which coincides with the observed value for ethanol. Therefore, we can not apply the same reasoning for the determination of nature of the transition in the present case.

It has been suggested by Mulliken that the  $\sigma^*$  MO of these molecules (especially those of a higher symmetry, for example,  $\text{NH}_3$  or  $\text{H}_2\text{O}$ ) may resemble very closely the  $3s$  AO of the central atom, and that they are both appropriate orbitals for describing the first molecular Rydberg states.<sup>13)</sup> It also seems probable that the two orbitals will interact with each other and form a mixed MO. The electronic transition to this MO will perhaps describe these upper states the most correctly insofar as the one-electron approximation is concerned. In fact, the  $(n+1)s$  AO is so large that it must interact very strongly with the AO's of other atoms in the same molecules. What we want to point out in this paper is

that the various characteristics of these bands can be explained well, at least in part, by the  $n \rightarrow \sigma^*$  type transition.

*The Institute for Solid State Physics  
The University of Tokyo  
Azabu, Tokyo*

### Appendix

For molecules of the  $\text{X}_1\text{OX}_2$  type, the  $\sigma^*$  orbitals for the  $\text{OX}_1$  bond and the  $\text{OX}_2$  bond are given by the following LCAO MO:

$$\sigma^*(\text{OX}_1) = a\phi_{\sigma_1} + b\phi_{\text{X}_1}$$

$$\sigma^*(\text{OX}_2) = a\phi_{\sigma_2} - b\phi_{\text{X}_2}$$

where  $\phi_{\sigma_1}$  and  $\phi_{\sigma_2}$  are the valence AO's directed along the two bonds and where  $\phi_{\text{X}_1}$  and  $\phi_{\text{X}_2}$  are the two valence AO's of  $\text{X}_1$  and  $\text{X}_2$ . The interaction between these two orbitals depends on the difference between their orbital energies and the interaction matrix element;

$$\beta = (\sigma^*(\text{OX}_1) | H | \sigma^*(\text{OX}_2)).$$

Inserting the explicit form, we have:

$$\beta = a^2 H_{\sigma_1 \sigma_2} - b^2 H_{\text{X}_1 \text{X}_2} - ab(H_{\sigma_1 \text{X}_2} - H_{\sigma_2 \text{X}_1})$$

All the terms contained in the equation except for  $H_{\sigma_1 \sigma_2}$  are between the AO's of atoms long distances apart and, hence, small.  $H_{\sigma_1 \sigma_2}$  is between AO's which belong to the same atom but which are orthogonal to each other with respect to the core potential. Therefore, we can see that all the terms in this equation must be small in absolute magnitude.

13) Personal discussion of H. Tsubomura with Professor Mulliken, 1962.